Intermittency of the density fluctuations and its influence on the radial transport in the boundary of J-TEXT*

Zhu Meng-Zhou(朱孟周)[a)b)†], Zhuang Ge(庄 革)[a)b)],
Wang Zhi-Jiang(王之江)[a)b)], and Pan Yuan(潘 垣)[a)b)]

[a)] *College of Electrical and Electronic Engineering, Huazhong University of Science and Technology, Wuhan* 430074, *China*
[b)] *Key Laboratory of Fusion and Advanced Electromagnetic Technology of Ministry of Education, Wuhan* 430074, *China*

(Received 17 August 2010; revised manuscript received 6 September 2010)

To improve the understanding of the turbulence intermittency, a detailed investigation of the intermittency of the density fluctuations has been performed in the boundary of J-TEXT. The intermittency of the density fluctuations and its influence on the radial transport are reported. The probability distribution functions of the density fluctuations are not scale-invariant, being inconsistent with the self-organized criticality hypothesis. The underlying dynamics of the intermittency are detected using the quiet-time statistical method. The probability distribution function of the quiet times shows double-power-law regions, indicating the existence of correlations between the successive burst events.

Keywords: intermittency, radial transport, J-TEXT

PACS: 52.70.Ds, 52.25.Gj, 52.55.Fa **DOI:** 10.1088/1674-1056/20/2/025204

1. Introduction

Decades of studies have shown that the cross-field transport is much higher than expected in the fusion research. Significant contributors to the anomalous transport are the intermittent burst events embedded in the fluctuations in the boundary of fusion devices.[1−3] Statistical analysis of the electrostatic fluctuations reveals that the intermittency is ubiquitous in nearly all the devices, such as tokamaks, stellarators, reversed-field pinches and linear devices.[4] The burst events, featuring higher pressure and radial velocities than the ambient plasma, can extend to the far scrape-off layer (SOL) and result in nearly flat density and temperature profiles there. Moreover, the burst events take about 50% of the radial transport in many fusion devices.[5−7] These observations question the traditional theoretical models based on the assumption that the fluctuations in the SOL are diffusive. More importantly, the burst events, taking a significant fraction of the radial transport, will increase the particle and energy loss, enhance the plasma-wall interaction, affect the boundary recycling, and consequently reduce the plasma confinement. Thus, studying the characteristics and understanding the source of the intermittency will be of great importance in finding effective measures to reduce its impact on the radial transport. A large number of experimental and theoretical studies have been devoted to these issues. However, the origin of the intermittency is still an open question.[8,9] A detailed review of the recent progress in understanding the intermittency can be found in the literature.[4,8] Experimental results obtained from different devices should be of great importance in revealing the universal and diverse characters of the intermittency, and hereafter, provide the possibility for deepening the understanding of the nature of the intermittency.

This paper presents a detailed description of the intermittency found in the boundary of J-TEXT and of their contributions to the radial transport; moreover, the dynamics between the successive burst events is detected in the SOL of J-TEXT. Emphasis is put on the characterization of the intermittency in the newly formed fusion device with the purpose of improving the understanding of the turbulence inter-

*Project supported in part by the National Basic Research Program of China (Grant No. 2008CB717805) and the National Natural Science Foundation of China (Grant No. 50907029).

†Corresponding author. E-mail: mengzhou99@126.com

© 2010 Chinese Physical Society and IOP Publishing Ltd

mittency. Besides, the new data will enrich the existing database constructed on the basic of different devices' results.

The remainder of this paper is organized as follows. The experimental set-up is described in Section 2. The experimental results are presented in Section 3, including the intermittency of the density fluctuations and the radial transport induced by the intermittency. Conclusions are given in the last section.

2. Experimental set-up

The J-TEXT,[10,11] formerly TEXT-U (Texas Experimental Tokamak Upgrade), whose major and minor radii are 1.05 m and 0.27 m, respectively, has been reconstructed and has been in operation since 2007. The experiments are carried out on J-TEXT with plasma current of 200 kA, toroidal magnetic field of 2.2 T and line average plasma density of 1.3×10^{19} m^{-3}. The typical discharge waveforms of plasma current, loop voltage, horizontal and vertical displacements of the plasma column are presented in Fig. 1. All data are taken in the flat top time of 200 ms (from 0.2 s to 0.4 s) in typical Ohmic hydrogen discharges with a limiter configuration.

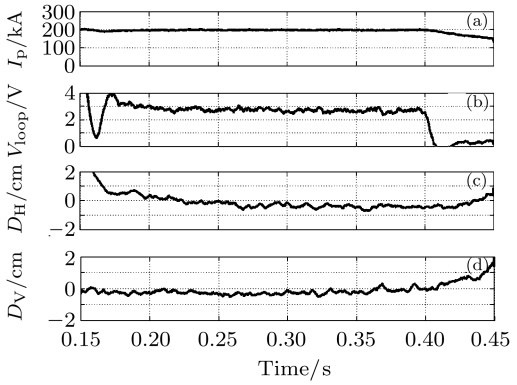


Fig. 1. Typical discharge waveforms of plasma current (a), loop voltage (b), horizontal displacement (c) and vertical displacement (d) of the plasma column.

The measurements are obtained from a Langmuir probe system mounted on the top of J-TEXT at 45° toroidally from the limiter. The probe system can be moved radially shot-by-shot. A square probe array with 3.5-mm spacing consists of four carbon tips with each tip 2 mm long and 1 mm in diameter. Two of the tips are operated as a double probe with a constant bias voltage of 180 V to record the ion saturation current (I_s) and the positive bias voltage (V_+). The other two tips are spaced poloidally to measure the floating potentials (denoted as V_{f1} and V_{f2}). Probe signals are acquired using 500-kHz digitizers with an accuracy of 16 bits. Local measurement of the density fluctuation, which is related to the particle transport, can be obtained from the I_s and the local electron temperature (T_e) using the formula $n_e \propto I_s T_e^{-1/2}$. In this paper, the fluctuation on T_e is assumed to be negligible. The poloidal electric field is $E_\theta = (V_{f1} - V_{f2})/d$, where d is the distance between the two tips spaced poloidally. The radial transport can be calculated using the formula $\Gamma_r = n_e V_r \propto I_s V_r$, where $V_r = E_\theta \times B_T/B_T^2$ and B_T is the toroidal magnetic field.

3. Experimental results

3.1. Intermittency of the density fluctuations

Intermittency means being patchy in space or bursty in time. A signature of the intermittency in measurement is the non-Gaussian probability distribution function (PDF).[12] The intermittency of the density fluctuations can be identified by direct analysis of the I_s signals. Figure 2 shows examples of the time-varying fluctuations of I_s and their corresponding PDFs at three different radial locations, where the fluctuations are normalized by their standard deviations. Inside the last closed flux surface (LCFS) shown in Fig. 2(a), there are lots of burst events embedded in the fluctuation signal. The frequency of the burst events, whose amplitudes are above 2.5 times the standard deviation, is about 2500 s^{-1}. The positive fluctuations are slightly more than negative ones, as revealed by the corresponding PDF shown in Fig. 2(b), where the PDF is asymmetric with a slight deviation from Gaussian distribution. Outside the LCFS shown in Fig. 2(c), the frequency of the burst events whose amplitudes are above 2.5 times the standard deviation, is about 3200 s^{-1}. The PDF shown in Fig. 2(d) reflects that the positive fluctuation is very close to a Gaussian distribution while the negative one is not. Deep into SOL, the fluctuation shown in Fig. 2(e) is dominated by more rare but larger positive bursts. The frequency of the burst events in which the amplitudes are greater than 2.5 times the standard deviation, increases to about 5200 s^{-1}. The PDF shown in Fig. 2(f) becomes strongly asymmetric with a pronounced tail towards the positive values. The enhanced relative amplitudes and the increased frequency of the burst events in the far SOL indicate that the intermittency becomes more important in the far SOL.

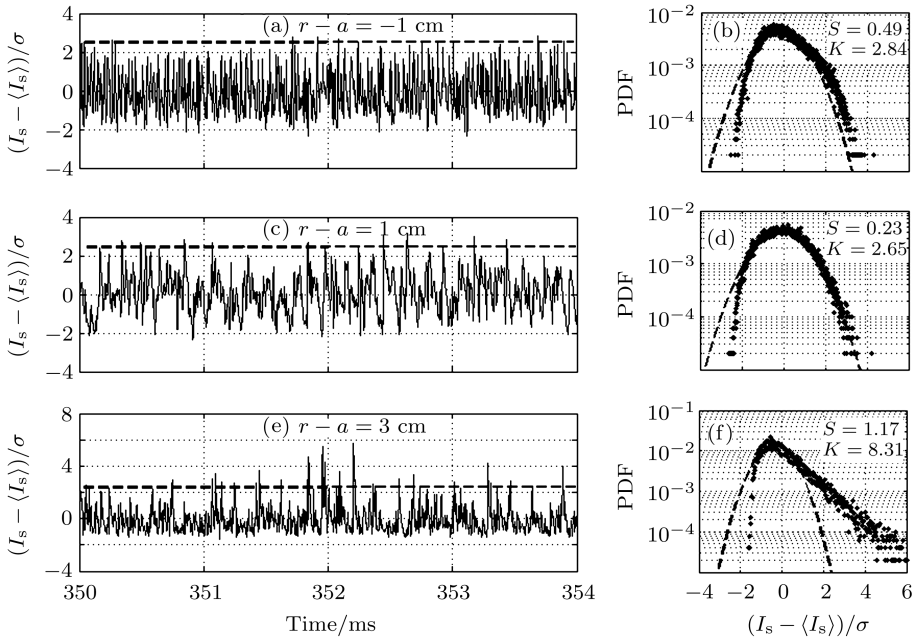


Fig. 2. Time evolutions of I_s fluctuations normalized by their standard deviations (panels (a), (c) and (e)), and the corresponding PDFs at three different radial locations (panels (b), (d) and (f)). The dotted lines indicate the amplitudes of the I_s fluctuations equal to 2.5 times their deviations (panels (a), (c) and (e)) and the best Gaussian fit to the PDFs (panels (b), (d) and (f)).

The deviation from Gaussian distribution can be quantified by the skewness and kurtosis of the fluctuation. For a signal x, the skewness S is defined as

$$S = \left\langle (x - \langle x \rangle)^3 \right\rangle / \sigma^3, \tag{1}$$

which describes the asymmetry of the PDF. The kurtosis K can be calculated in the following way:

$$K = \left\langle (x - \langle x \rangle)^4 \right\rangle / \sigma^4, \tag{2}$$

which describes the tail weight with respect to the central distribution. For a Gaussian signal, the skewness and the kurtosis are zero and three, respectively. Figure 3 shows the radial dependences of skewness and kurtosis of the density fluctuations. At each radial position, data averaging is achieved by five identical shots with 200-ms length (from 0.2 s to 0.4 s, 100000 data points). Both the skewness and the kurtosis are almost invariable (about 0.5 and 3, respectively) near the LCFS while tend to increase in the far SOL, confirming that the intermittency becomes stronger in the far SOL than that near the LCFS. This is in accordance with the phenomena observed in Fig. 2.

To gain further insight into the nature of the intermittency, a conventional power spectrum of the density fluctuation is obtained by Fourier analysis. In the analysis, the data set obtained from a typical discharge is broken into twenty-four non-overlapping sub-blocks, and each sub-block has 4096 data points. Figure 4(a) shows the power spectrum of the I_s fluctuation in shot 11020. There are no significant peaks in the spectrum, indicating that the density fluctuation is not dominated by periodic signals. The spectrum breaks at about 7 kHz and 25 kHz. The shape of the spectrum is divided into three regions which can be described by power-law dependences of the type $S(f) \propto f^{-m}$, a flat region at low frequencies, an intermediate one with a spectral index of about $m = 1$, and a steep one with exponent m close to 2. A similar shape of the power spectrum has also been observed in the edge of J-TEXT in the density fluctuations.

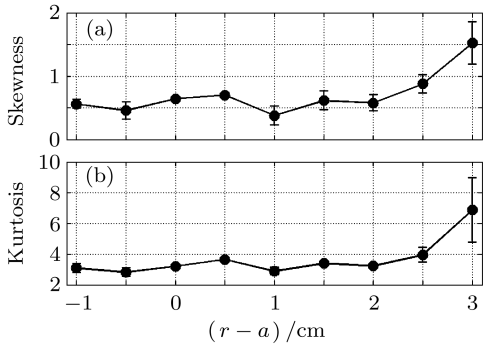


Fig. 3. Radial profiles of skewness (a) and kurtosis (b) of the density fluctuations. Error bars indicate the standard deviations of the mean from five reproducible discharges for each location.

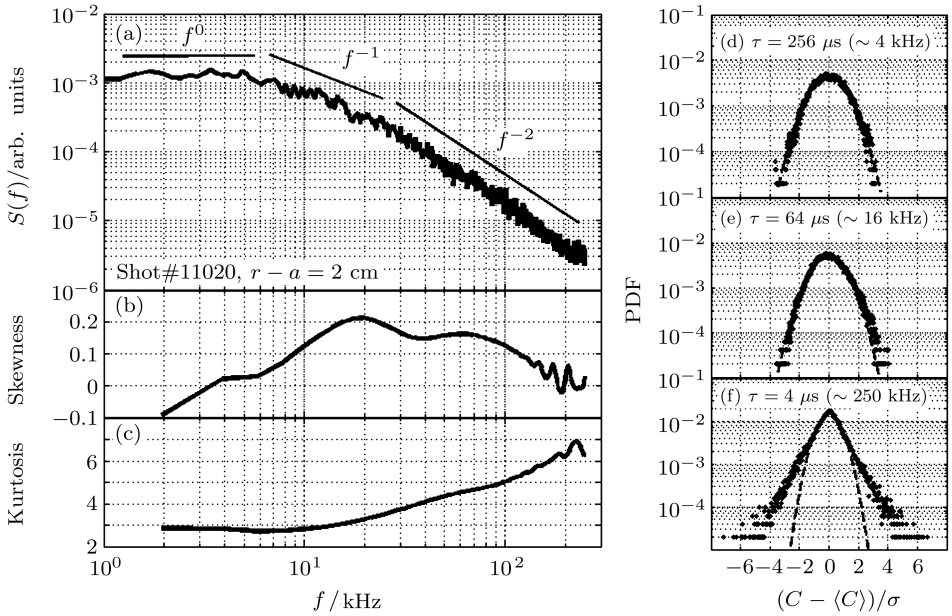


Fig. 4. Power spectrum of the I_s fluctuation (a), skewness and kurtosis of the decomposition of the I_s signal versus frequencies (panels (b) and (c)), and PDFs of the I_s fluctuation at three different frequencies (panels (d), (e) and (f)). The dotted lines indicate the best Gaussian fit to the PDFs (panels (d), (e) and (f)).

The intermittency corresponding to the different regions mentioned above can be quantified by calculating the skewness and kurtosis of the decomposition of I_s signals at the corresponding frequencies. For this, the wavelet transform is applied to obtain a set of wavelet coefficients for each time scale τ, where $\tau = 1/f$. The wavelet transform is a time-frequency transform, which has the form

$$C(\tau, s) = \frac{1}{\sqrt{\tau}} \int_{-\infty}^{+\infty} I_s(t) \psi \left(\frac{t-s}{\tau} \right) \mathrm{d}t, \qquad (3)$$

where C is the wavelet coefficients and ψ is the wavelet function. This allows us to obtain the decomposition of the I_s signal at the scale τ as a function of the time parameter s. Here the Morlet wavelet is used for the analysing function ψ. Wavelet coefficients represent the time behaviour of characteristic fluctuations at each scale τ. The skewness S_τ and kurtosis K_τ of the density fluctuation at each time scale are the normalized third and fourth order moments of wavelets coefficients for the corresponding scales. The corresponding formulas are

$$S_\tau = \left\langle \left(C(\tau) - \langle C(\tau) \rangle \right)^3 \right\rangle / \sigma_\tau^3 \qquad (4)$$

and

$$K_\tau = \left\langle \left(C(\tau) - \langle C(\tau) \rangle \right)^4 \right\rangle / \sigma_\tau^4, \qquad (5)$$

where σ_τ is the standard deviation of wavelets coefficients at the scale τ. Figures 4(b) and 4(c) show the variations of the skewness S_τ and kurtosis K_τ with frequencies. The skewness tends to increase from –0.1 to 0.2 with frequencies up to 20 kHz, and has a maximum value near the frequency of 20 kHz, suggesting a maximum positive deviation of the rescaled fluctuations at this frequency. In the range of 20 kHz and 250 kHz, the skewness tends to decrease from 0.2 to about 0, indicating that the deviation becomes smaller with increasing frequencies. The kurtosis is about zero at frequencies up to about 10 kHz. When the frequencies are above 10 kHz, an increase of the kurtosis with increasing frequencies is found, indicating that the intermittency of the density fluctuation is more obvious at high frequencies. The variations of skewness and kurtosis with frequencies indicate that the PDFs of the density fluctuations at the three different power-law regions mentioned above are near-Gaussian, positive skewed, and more stretched, respectively. Examples of these behaviours are presented in Figs. 4(d), 4(e) and 4(f), which show that the PDFs are near-Gaussian at low frequencies (4 kHz and 16 kHz) and tend to develop strong tails at higher frequencies (250 kHz). These results indicate that the density fluctuations are not scale-invariant.

Another important issue is the underlying dynamics of the intermittency. Quiet-time statistics[13,14] is an approach to probe the dynamics between the successive burst events, which allows the extraction of information of the long-range correlation by measur-

ing the quiet times between the events. The statistics of the quiet times is somewhat related to the waiting times, but the quiet times can be shown not to suffer from the same shortcomings as their relatives. First, it is important to measure quiet times instead of waiting times if we intend to separate the correlations induced by the drive and the ones induced by the dynamics. Second, the distribution of the quiet times between all burst events in the system essentially reflects the statistics of the drive.[13] Based on the utility of the quiet-time statistics, the method is performed on the I_s signal in the SOL of J-TEXT. In the analysis, a reference level of 2.5 times deviation of the I_s fluctuation is used to measure the quiet times between the successive burst events. The PDF of the quiet times is shown in Fig. 5, which displays two distinct power law regions ($P(\tau_q) \propto \tau_q^{-\gamma}$) with the power law exponents of $\gamma = 1.05 \pm 0.06$ and $\gamma = 2.29 \pm 0.18$, respectively. The result implies the existence of correlation between the successive burst events.

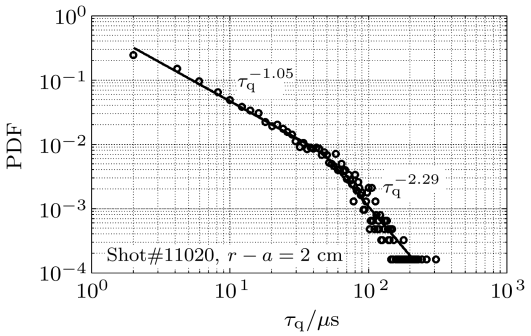
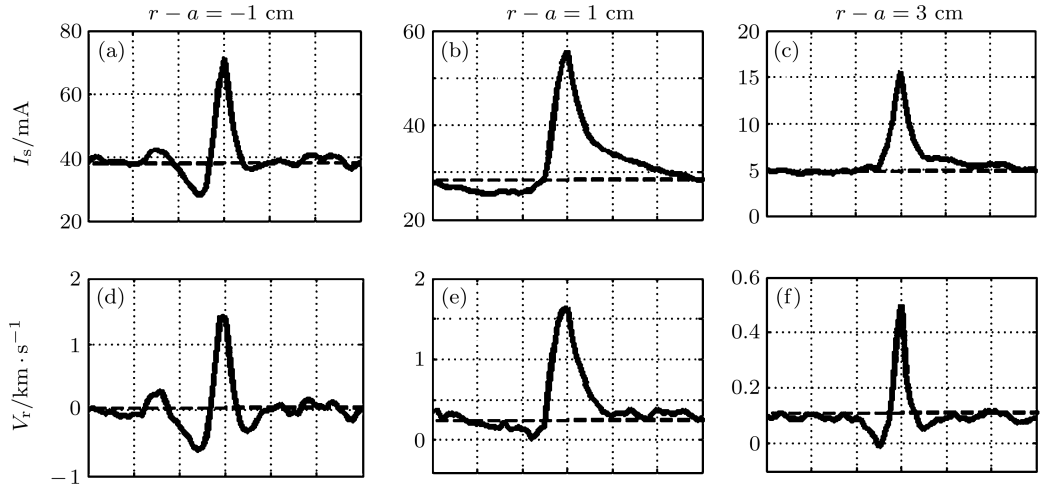


Fig. 5. PDF of the quiet times. Power-law fit is shown by the solid lines.

3.2. Transport induced by intermittency

The intermittency of the radial transport can be characterized by measuring the burst events of I_s, V_r, and I_sV_r using the conditional averaging analysis.[15,16] By setting a certain level threshold, normally several times the standard deviation, the burst events can be selected from the time series signals. Conditional averaging is achieved by recording a certain number of points around the maxima of each event and then accumulating and averaging the selected events. If both the selection criterion and the selected object are performed on the same signal, it is called "auto-conditional averaging". If the selection criterion is made on one signal while the averaging is done on another, it is called "cross-conditional averaging".

Figure 6 displays the conditional average of I_s, V_r, and I_sV_r at three different radial locations, where I_sV_r is used to qualify the particle transport. The intermittent structures of I_s are shown in Fig. 6 (panels (a)–(c)), which are selected using auto-conditional average for the threshold of $(I_s - \langle I_s \rangle)/\sigma = 2.5$. The maximum values of the burst events at the three different radial locations are 70, 56, and 15 mA, respectively. The corresponding mean values of I_s are 37, 28, and 5 mA, respectively. The maximum values are about two times the corresponding mean values near the LCFS, while deep into SOL, the ratio increases to three. Although both the maximum values and the mean values decrease outwards along the radius, the burst events still feature higher density than the ambient plasma.



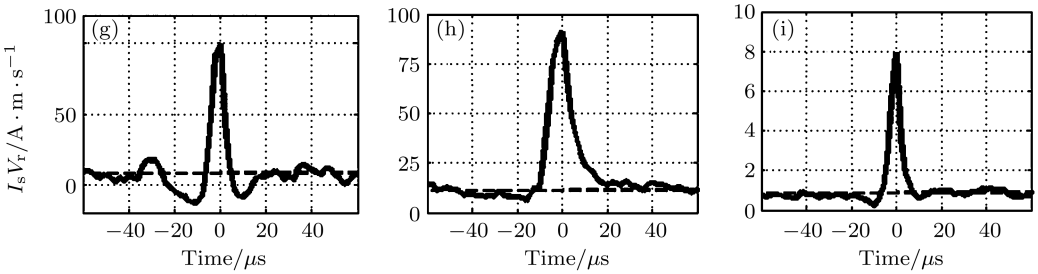


Fig. 6. Conditional averaging of I_s, V_r, and I_sV_r at three different radial locations for the same threshold of $(I_{sat} - \langle I_{sat}\rangle)/\sigma = 2.5$. The dotted lines indicate the mean values of the corresponding signals.

The intermittent structures of V_r are obtained using cross-conditional average with the same threshold mentioned above. A comparison of V_r at the three different radial locations is shown in Fig. 6 (panels (d), (e), and (f)). The maximum radial velocities of the burst events are 1.5, 1.6, and 0.5 km/s, respectively. The corresponding mean velocities of V_r are 0.02, 0.2, and 0.1 km/s, respectively. Although the maximum radial velocities of the burst events decrease with the radius, these data indicate that the velocities of the burst events are essentially larger than the corresponding mean velocities.

The intermittent structures of I_sV_r at the same locations are shown in Fig. 6 (panels (g), (h), and (i)), which are selected using cross-conditional average at the same threshold. The maximum values of the burst events are about 100, 88, and 8 Am/s, respectively. The corresponding mean values of I_sV_r are 7, 12, and 0.8 Am/s, respectively. The maximum values of the burst events are much higher than the corresponding mean values of I_sV_r, implying that the burst events have a significant impact on the radial transport.

The radial transport induced by the intermittency can be calculated by using

$$\langle \Gamma\rangle_{\rm int}/\langle \Gamma\rangle_{\rm tot} = \langle I_sV_r\rangle_{\rm int}/\langle I_sV_r\rangle_{\rm tot}, \qquad (6)$$

where $\langle I_sV_r\rangle_{\rm int}$ represents the radial transport carried by the burst event, and $\langle I_sV_r\rangle_{\rm tot}$ represents the total radial transport. The burst events, where amplitudes are above 2.5 times standard deviation of the I_sV_r fluctuations, are responsible for 25%–45% of the radial transport in the boundary of J-TEXT.

4. Discussion and conclusion

The experimental results mentioned above reveal that the intermittency is ubiquitous in the boundary of J-TEXT. The PDFs of the density fluctuations deviate from pure Gaussain distribution, particularly in the far SOL. The cause for the breakdown of the Gaussain distribution is considered to be the existence of intermittency in the fluctuations, which is considered as a consequence of the underlying turbulence dynamics.[14] Among the models proposed to describe the turbulence dynamics in the fusion research, the self-organized-criticality (SOC) models have been widely used owing to some properties of the plasma, like the burst behaviour, power-law decay in fluctuation spectra, long-range spatial and temporal correlation through scale invariance.

In the experiments of this paper, the power spectrum of the density fluctuation shows three power-law regions. The presence of the f^{-1} region gives an indication of the avalanche interactions. Besides, the power-law dependences of the spectrum reflect the self-similar behaviour of the density fluctuation in the three different regions. The power-law spectrum and the intermittency behaviour of the density fluctuations are consistent with the SOC hypothesis. However, further research reveals that the PDFs of the density fluctuations are not scale-invariant. This is inconsistent with the self-similar property of the SOC hypothesis.[17]

In order to get insights into the underlying dynamics of the intermittency, the PDF of the quiet times for density fluctuations is investigated, which has been found to exhibit double-power-law decay. This decay is in contrast with the predictions of the standard SOC model, the Bak–Tang–Wiesenfeld (BTW) model, which predicts an exponential decay instead. However, as mentioned in Ref. [18] some authors have conjectured that other SOC models, including the running sandpile, could allow for a power-law decay for the PDF of quiet times in laboratory plasmas. Anyway, the occurrence of the power-law decay in the distribution of quiet times indicates the existence of correlations between the successive burst

events.

The burst events, featuring higher density and radial velocity than the surrounding plasma, are responsible for 25%–45% of the radial transport in the boundary of J-TEXT. Although the ratio is smaller than the results observed in many other devices,[5,6] the burst events still have a significant impact on the radial transport. Experiments in the boundary of DIII-D and SUNIST showed that the particle content of the burst events and their frequency increase with the local density.[5,19] Thus, there is evidence to believe that the burst events in J-TEXT will have a greater impact on the radial transport with increasing density. The relevant experiments are underway.

In summary, the intermittency of the density fluctuations has been characterized in the boundary of J-TEXT. Results show that the intermittency is ubiquitous both near the LCFS and in the far SOL. The positive fluctuations are slightly more than the negative ones near the LCFS, while deep into SOL, the fluctuations are dominated by more rare but larger positive peaks. The density fluctuation is not dominated by periodic signals, and its power spectrum shows three power-law regions. Moreover, the wavelet decomposition reveals that the PDFs of the density fluctuations are not scale-invariant, being inconsistent with the SOC hypothesis. Quiet-time statistics shows that the PDF of the quiet times exhibits double-power-law regions, indicating the existence of correlations between the successive burst events. Particularly, the conditional averaging reveals that the burst events featuring higher density and radial velocities than the surrounding plasma have a significant impact on the radial transport. The fraction of the radial transport carried by the burst events is about 25%–45% in the boundary of J-TEXT.

Acknowledgements

Discussions with K. Gentle are acknowledged. The authors would like to thank the members of the J-TEXT team for their collaboration and helpful discussion in the experiments.

References

[1] Boedo J A 2009 *J. Nuclear Mater.* **390–391** 29

[2] Boedo J A, Rudakov D, Moyer R, Krasheninnikov S, Whyte D, McKee G, Tynan G, Schaffer M, Stangeby P, West P, Allen S, Evans T, Fonck R, Hollmann E, Leonard A, Mahdavi A, Porter G, Tillack M and Antar G 2001 *Phys. Plasmas* **8** 4826

[3] Happel T, Greiner F, Mahdizadeh N, Nold B, Ramisch M and Stroth U 2009 *Phys. Rev. Lett.* **102** 255001

[4] Zweben S J, Boedo J A, Grulke O, Hidalgo C, LaBombard B, Maqueda R J, Scarin P and Terry J L 2007 *Plasma Phys. Control Fusion* **49** S1

[5] Boedo J A, Rudakov D L, Moyer R A, McKee G R, Colchin R J, Schaffer M J, Stangeby P G, West W P, Allen S L, Evans T E, Fonck R J, Hollmann E M, Krasheninnikov S, Leonard A W, Nevins W, Mahdavi M A, Porter G D, Tynan G R, Whyte D G and Xu X 2003 *Phys. Plasmas* **10** 1670

[6] Cheng J, Yan L W, Hong W Y, Zhao K J, Lan T, Qian J, Liu A D, Zhao H L, Liu Y, Yang Q W, Dong J Q, Duan X R and Liu Y 2010 *Plasma Phys. Control Fusion* **52** 055003

[7] Wang W H, Yu C X, Wen Y Z, Xu Y H, Ling B L, Gong X Z, Liu B H and Wan B N 2001*Chin. Phys.* **10** 139

[8] Krasheninnikov S I, D'Ippolito D A and Myra J R 2008 *J. Plasma Phys.* **74** 679

[9] Xu G S, Naulin V, Fundamenski W, Hidalgo C, Alonso J A, Silva C, Goncalves B, Nielsen A H, Juul Rasmussen J, Krasheninnikov S I, Wan B N, Stamp M and JET EFDA Contributors 2009 *Nucl. Fusion* **49** 092002

[10] Zhuang G, Ding Y H, Zhang M, Yu K X, Zhang X Q, Wang Z J, Hu X W and Pan Y 2009 *Plasma Sci. Technol.* **11** 439

[11] Yang Z J, Zhuang G, Hu X W, Zhang M, Qiu S S, Wang Z J, Ding Y H and Pan Y 2009 *Fusion Eng. Design* **84** 2093

[12] Carter T A 2006 *Phys. Plasmas* **13** 010701

[13] Sanchez R, Newman D E, Ferenbaugh W, Carreras B A, Lynch V E and van Milligen B Ph 2002 *Phys. Rev.* E **66** 036124

[14] Lynch V E, Carreras B A, Sanchez R, LaBombard B, van Milligen B Ph and Newman D E 2005 *Phys. Plasmas* **12** 052304

[15] Filippas A V, Bengston R D, Li G X, Meier M, Ritz Ch P and Powers E J 1995 *Phys. Plasmas* **2** 839

[16] Antar G Y, Krasheninnikov S I, Devynck P, Hollmann E M, Boedo J A, Luckhardt S C and Conn R W 2001 *Phys. Rev. Lett.* **87** 065001

[17] Antoni V, Carbone V, Cavazzana R, Regnoli G, Vianello N, Spada E, Fattorini L, Martines E, Serianni G, Spolaore M, Tramontin L and Veltri P 2001 *Phys. Rev. Lett.* **87** 045001

[18] Spada E, Carbone V, Cavazzana R, Fattorini L, Regnoli G, Vianello N, Antoni V, Martines E, Serianni G, Spolaore M and Tramontin L 2001 *Phys. Rev. Lett.* **86** 3032

[19] Wang W H, He Y X, Gao Z, Zeng L, Zhang G P, Xie L F and Feng C H 2004 *Chin. Phys.* **13** 2091